

## The Effect of Electrolyte Selection on the Electrochemical Performance of Nano-Size Anatase TiO<sub>2</sub> as Anode Materials for Solidum-Ion Batteries

Fei Gao<sup>1</sup>, Maosong Fan<sup>1</sup>, Baogui Tian<sup>2</sup>, Kangkang Wang<sup>1,\*</sup>, Zhaolin Li<sup>1</sup>, Hailei Zhao<sup>2,\*</sup>

<sup>1</sup>State Key Laboratory of Operation and Control of Renewable Energy and Storage Systems, China Electric Power Research Institute, Beijing, 100192, China

<sup>2</sup>School of Materials Science and Engineering, University of Science and Technology Beijing, Beijing 100083, China

\*corresponding author

**Keywords:** sodium-ion battery, anode, anatase TiO<sub>2</sub>, electrolyte

**Abstract:** Nano-size anatase TiO<sub>2</sub> is identified as an promising anode material for sodium-ion batteries. However, the chemical compatibility of nano-size TiO<sub>2</sub> anode and the liquid electrolytes and its effects on discharge capacity and rate capability are still unknown. In this work, NaClO<sub>4</sub>-based and NaPF<sub>6</sub>-based liquid electrolytes are selected to study their effect on the electrochemical performance of anatase TiO<sub>2</sub> anode. Our result demonstrates that NaClO<sub>4</sub>-based electrolyte leads to better cycling performance as compare to the NaPF<sub>6</sub>-based electrolyte. The discharge specific capacity for anatase TiO<sub>2</sub> with NaClO<sub>4</sub>-based electrolyte at 1 C remains about 130 mAh g<sup>-1</sup> after 150 cycles, whereas the specific capacity drastically dropped to 35 mAh g<sup>-1</sup> in NaPF<sub>6</sub>-based electrolyte. Furthermore, anatase TiO<sub>2</sub> anode also shows better rate capability in NaClO<sub>4</sub>-based electrolyte than in NaPF<sub>6</sub>-based electrolyte.

### 1. Introduction

Sodium-ion battery has been recognized as an promising and cost effective system for next-generation large-scale electrical energy storage, due to the abundance and easy access of sodium-derived compounds in earth. For the cathode side, many materials, including layered transition metal oxides [1–4], three-dimensional Na<sub>0.44</sub>MnO<sub>2</sub> [5,6], and Prussian blue [7] have been demonstrated as promising candidates with fairly high specific capacity. As for the anode side, many studies have focused on carbon-derived materials owing to their low redox potential, good structure stability and low materials and manufacturing cost. Graphite, traditionally used in commercial lithium ion batteries, is unfortunately electrochemically inactive for sodium-ion batteries due to the limited channel size in graphite as compared to the size of sodium ion [8]. Other types of carbon-based materials, such as amorphous carbon [9] and carbon nanofibers [10], were recently demonstrate to have superior capacities, attributing to their enlarged layer spacing in their disordered structures. However, the relatively low operating potential (ca. 0.1 V vs. Na/Na<sup>+</sup>) of these hard carbon anodes can easily lead to sodium dendrites growth during operation, rising additional concerns on battery safety.

Besides carbon-based materials, recent studies have evidenced that TiO<sub>2</sub>-based materials, including TiO<sub>2</sub>(B) [11], anatase TiO<sub>2</sub> [12–14], and hollandite-type TiO<sub>2</sub> [15], can be utilized to store Na ions and are potentially useful as anode materials for sodium ion batteries with high reversible capacity and moderate operating potential. However, the chemical compatibility of TiO<sub>2</sub> anodes and different liquid electrolytes and its effect on electrochemical performance of the cell are still unclear in the field. In the work, we studied the electrochemistry performance of nano-size anatase TiO<sub>2</sub> (25nm) in two different liquid electrolytes. It is concluded that the NaClO<sub>4</sub>-based electrolyte offers better compatibility with TiO<sub>2</sub> anode and shows better cycling performance as compared to NaPF<sub>6</sub>-based electrolyte.

## 2. Experimental methods

We strongly encourage authors to use this document for the preparation of the camera-ready. Please follow the instructions closely in order to make the volume look as uniform as possible.

Please remember that all the papers must be in English and without orthographic errors.

Do not add any text to the headers (do not set running heads) and footers, not even page numbers, because text will be added electronically.

For a best viewing experience the used font must be Times New Roman, on a Macintosh use the font named times, except on special occasions, such as program code.

### 2.1. Structure and morphology characterization

The crystal structure of the synthesized samples was characterized by X-ray powder diffraction (XRD, Rigaku) in the range of  $5^{\circ}$ – $80^{\circ}$ , with  $\text{Cu } \alpha$  ( $1.54 \text{ \AA}$ ) radiation.

### 2.2. Cell assembly and testing

The electrodes were prepared with a composition of 70 wt.% active materials, 20 wt.% Super P (a conductive additive), and 10 wt.% PVDF as a binder. The electrodes were then dried in an oven at  $80^{\circ}\text{C}$  for more than 12 h. Charge-discharge tests were performed using CR2032-type coin cells. Fresh metal Na was used as the counter electrode, and glass microfiber filters (GF/D Whatman) were used as separators. Two different electrolytes were prepared for cell testing, including 1) 1 M solution of  $\text{NaClO}_4$  in ethylene carbonate (EC) and dimethyl carbonate (DMC) (1:1 in volume) with 5% fluoroethylene carbonate additive (5% in volume); 2) 1M solution of  $\text{NaPF}_6$  in ethylene carbonate (EC) and dimethyl carbonate (DMC) (1:1 in volume). Cell assembly was completed in an argon-filled glove box.

## 3. Results and discussion

### 3.1. Characterization of the structure and micromorphology

XRD pattern of the as-synthesized  $\text{TiO}_2$  sample is illustrated in Fig. 1. Peaks centered at  $25.3^{\circ}$ ,  $37.8^{\circ}$ ,  $48^{\circ}$ ,  $53.8^{\circ}$ ,  $55^{\circ}$ ,  $62.7^{\circ}$ ,  $68.7^{\circ}$ , and  $70^{\circ}$  match well with typical tetragonal anatase  $\text{TiO}_2$  (JCPDS NO.21–1272).

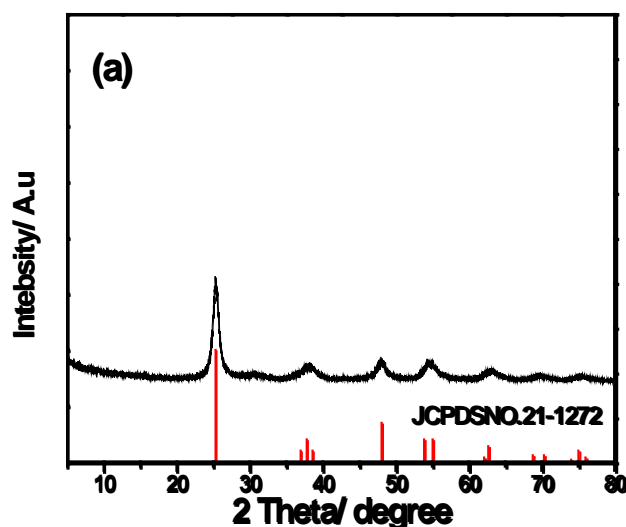


Figure 1 XRD pattern of the P25  $\text{TiO}_2$  sample.

### 3.2. Electrochemical properties of the TiO<sub>2</sub> samples

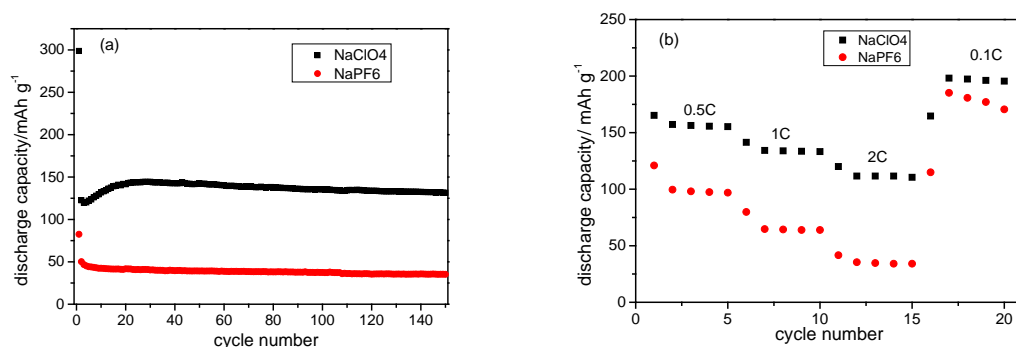


Figure 2. Electrochemical performances: (a) discharge capacity at 1C; (b) rate performance.

The cycling performance of the anatase TiO<sub>2</sub> anode at 1C in the two different electrolytes are shown in Fig. 2a. Comparatively, anatase TiO<sub>2</sub> with NaClO<sub>4</sub>-based electrolyte exhibits higher discharge capacity than that with NaPF<sub>6</sub>-based electrolyte. The initial discharge capacity of the anatase TiO<sub>2</sub> are 298.7 and 82.5 mAh·g<sup>-1</sup> in NaClO<sub>4</sub>-based and NaPF<sub>6</sub>-based electrolytes, respectively, and, the discharge capacity remains around 131.5 and 35.2 mAh·g<sup>-1</sup> after 150 cycles. Fig. 2b reveals the rate capability of the anatase TiO<sub>2</sub> electrode at rates of 0.1C, 0.5C, 1C, and 2C. The electrode also exhibits capacity advance in the NaClO<sub>4</sub> solution electrolyte. The average discharge capacity can still remain at 111/34.3 mAh·g<sup>-1</sup> even at 2 C in the two electrolytes. When the current density drops back to 0.1 C, the discharge capacity can restore to about 196/177 mAh·g<sup>-1</sup>.

### 4. Conclusion

In summary, this study highlights that electrolytes can greatly affect the electrochemical performance of nano-size anatase TiO<sub>2</sub> anode in sodium ion batteries. Anatase TiO<sub>2</sub> delivers rather high reversible capacity, stable cyclic performance and good rate capability in the NaClO<sub>4</sub>-based electrolyte as compared to its performance in NaPF<sub>6</sub>-based electrolyte.

### Acknowledgements

This research was financially supported by the Science and Technology Projects of State Grid Corporation (“Research on key technology of low-strain layered oxides for long-life Na-ion batteries”, No. DG71-16-027).

### References

- [1] R. Berthelot, D. Carlier, C. Delmas, *Nat. Mater.* 10 (2011) 74–80.
- [2] N. Yabuuchi, M. Yano, H. Yoshida, S. Kuze, S. Komaba, *J. Electrochem. Soc.* 160 (2013) A3131–A3137.
- [3] J. Zhao, J. Xu, D.H. Lee, N. Dimov, Y.S. Meng, S. Okada, *J. Power Sources* 264 (2014) 235–239.
- [4] N. Yabuuchi, M. Kajiyama, J. Iwatate, H. Nishikawa, S. Hitomi, R. Okuyama, R. Usui, Y. Yamada, S. Komaba, *Nat. Mater.* 11 (2012) 512–517.
- [5] Y. Cao, L. Xiao, W. Wang, D. Choi, Z. Nie, J. Yu, L. V. Saraf, Z. Yang, J. Liu, *Adv. Mater.* 23 (2011) 3155–3160.
- [6] F. Sauvage, L. Laffont, J.M. Tarascon, E. Baudrin, *Inorg. Chem.* 46 (2007) 3289–3294.

- [7] Y. Lu, L. Wang, J. Cheng, J. B. Goodenough, *Chem. Commun.* 48 (2012) 6544–6546.
- [8] K. Tang, L. Fu, R. J. White, L. Yu, M.M. Titirici, M. Antonietti, J. Maier, *Adv. Energy Mater.* 2 (2012) 873–877.
- [9] J. Zhao, L. Zhao, K. Chihara, S. Okada, J.-i. Yamaki, S. Matsumoto, S. Kuze, K. Nakane, *J. Power Sources* 244 (2013) 752–757.
- [10] W. Luo, J. Schardt, C. Bommier, B. Wang, J. Razink, J. Simonsen, X. Ji, *J. Mater. Chem. A* 1 (2013) 10662–10666.
- [11] J. P. Huang, D. D. Yuan, H. Z. Zhang, Y. L. Cao, G. R. Li, H. X. Yang, X. P. Gao, *RSC Adv.* 3 (2013) 12593–12597.
- [12] L. Wu, D. Buchholz, D. Bresser, L. Gomes Chagas, S. Passerini, *J. Power Sources* 251 (2014) 379–385.
- [13] K. T. Kim, G. Ali, K. Y. Chung, C. S. Yoon, H. Yashiro, Y. K. Sun, J. Lu, K. Amine, S. T. Myung, *Nano. lett.* 14 (2014) 416–422.
- [14] Y. Xu, E. M. Lotfabad, H. Wang, B. Farbod, Z. Xu, A. Kohandehghan, D. Mitlin, *Chem. Commun.* 49 (2013) 8973–8975.